



# Numerical Study of Forced Air Cooling of a Heated Porous Foam Pyramid Array

K. Anderson<sup>†</sup>, M. Shafahi and A. Gutierrez

*California State Polytechnic University at Pomona, Mechanical Engineering, Non-linear FEA/CFD Multiphysics Simulation Laboratory, Pomona, CA, 91768, USA*

<sup>†</sup>Corresponding Author Email: [kranderson1@cpp.edu](mailto:kranderson1@cpp.edu)

(Received January 6, 2014; accepted November 18, 2014)

## ABSTRACT

The current study employs CFD to study the forced air cooling of a pyramid shaped porous foam absorber. Herein, a three by three (3×3) array of porous foam absorbers heated with an external heat flux is modeled using the differential equations governing heat and fluid flow through porous media based on the Brinkman-Darcy flow equations and an effective thermal conductivity to account for the porous medium. The numerical simulations are carried out using the COMSOL commercial Computational Fluid Dynamics (CFD) Finite Element based software package. The results of this verification exercise were within 18% of the prior numerical results and within 14% of the archived measured results. Typical results for the velocity and temperature profiles within the porous foam absorbers are shown. A comparison of Nusselt number between our CFD simulations and the heat transfer theory is plotted, showing agreement on the order of 11%. A parametric study involving heat flux, cooling air inlet velocity, porous foam porosity, and porous foam permeability showed that there is a relationship between porosity and the temperature distribution within the porous media. The primary finding of our study is that the more porous the foam absorber media is, the more dependent the effective thermal conductivity is on the thermal conductivity of the fluid used for cooling. If the fluid is air, which has a very low thermal conductivity, the effective thermal conductivity is decreased as the porosity increases, thus diminishing removal of heat from the foam array via the cooling air stream. Based on the parametric study, the best case operating conditions which may allow the pyramidal foam absorber to stay within the max allowable temperature are as follows: porosity = 0.472, inlet air cooling velocity = 50 m/s.

**Keywords:** Porous media; Computational fluid dynamics; Forced convection; Heat transfer.

## NOMENCLATURE

|           |                                |                    |                     |
|-----------|--------------------------------|--------------------|---------------------|
| $C_{ps}$  | specific heat of solid         | $\alpha$           | thermal diffusivity |
| $C_{pf}$  | specific heat of fluid         | $\varepsilon$      | porosity            |
| $d$       | sphere diameter                | $\mu$              | dynamic viscosity   |
| $g$       | gravitational constant         | $\nu$              | kinematic viscosity |
| $k_s$     | thermal conductivity of solid  | $\rho_s$           | solid density       |
| $k_f$     | thermal conductivity of fluid  | $\rho_f$           | fluid density       |
| $k_{eff}$ | effective thermal conductivity | $\kappa$           | permeability        |
| $Nu$      | Nusselt number                 | <b>Subscripts:</b> |                     |
| $Pe$      | Peclet number                  | $f$                | Fluid               |
| $T$       | temperature                    | $s$                | Solid               |
| $u, v, w$ | $x, y, z$ velocity components  | $eff$              | Effective           |
| $V$       | velocity vector                |                    |                     |

## 1. INTRODUCTION

Heat transfer and fluid flow in porous media

continues to find applications within the different branches of engineering as outlined by Narasimhan (2012). Specifically, per Cekmer et al. (2012) heat

transfer in porous media has been found to be of interest in the fields involving oil recovery, water supply management, nuclear waste disposal, and ground water flow modeling. This topic has also been the subject of various academic research based studies (Narasimhan 2012; Dukman and Chen 2007) which include the derivations of fundamental equations used in the analysis of porous media flow and heat transfer. Heat transfer in porous media has been extensively studied by others for a specific type of material known as metal foam (Boomsma and Poulikakos 2000; Zhao *et al.* 2005; Bhattacharya *et al.* 2002; Phanikumar and Mahajan 2002; Hsieh *et al.* 2004; Ghosh 2009; Kopanidis *et al.* 2010). Metal foam finds extensive use in the automotive and biomedical fields. Metal foam is ideal for use in these fields as it has a high strength to weight ratio and has the ability to absorb energy from impacts. Dukhan and Chen (2007) provide a modeling and experimental study for the heat transfer in open celled aluminum foam exposed to forced convection with low thermally conductive air.

For the current study, however, metal foam would not be a suitable replacement for polyurethane pyramidal absorbers (found to be the most commonly used material) used in anechoic chambers as the metal foam is a perfect reflector and would not be capable of absorbing electromagnetic/radio frequency waves. Presently it would appear that there is a lack of studies available in the literature involving the numerical simulation and testing of heat transfer characteristics in porous foam polyurethane pyramidal absorbers. Thus the current investigation seems warranted. Our study is related to that of Watanabe *et al.* (2007), who have studied and performed a thermal analysis on electromagnetic waves on a single pyramidal foam absorber used in anechoic chambers. The geometry used by Watanabe *et al.* (2007), and hence modified for the current CFD based study is shown in Fig. 1.

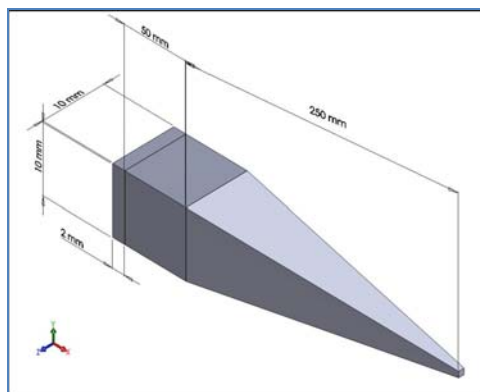


**Fig. 1. Single pyramidal absorber.**

Figure 1 shows the pertinent dimensions of a single porous foam pyramid shaped absorber. Such absorbers are typically used in the noise and radio frequency industries. The cooling air is blown into the porous media from the base of 10 mm by 10 mm and allowed to flow through the heated absorber. The heat transfer thermal control concept

envisioned herein is to cool the foam by blowing air through its many pores.

The study of Watanabe *et al.* (2007) solved the governing differential equations and experimentally determined the temperature profile along the centerline of the absorber and compared the results, which were within 22% of the measured results. The study concluded that the calculated and measured results agreed well and confirmed the validity of the coupled method used in their study.

In this present study, the work of Watanabe *et al.* (2007) is used to Verify and Validate (V&V) the CFD model used in our current work. Following the V&V effort, a CFD model of a 3 by 3 array of pyramidal foam absorbers was built. A parametric study is performed using the CFD model of the 3 by 3 array model in order to characterize the influence of certain parameters (such as porosity,  $\epsilon$  and permeability,  $\kappa$ ) have on the system in terms of temperature gradient along the centerline and Nusselt number (dimensionless heat transfer coefficient). To this end, the results from the CFD model of the 3 by 3 array of absorbers are compared with the analytical solution proposed by Bejan (1994) for a plane wall with constant heat flux. The data from this work and the results found from the analytical solution are in excellent agreement.

## 2. PROBLEM DESCRIPTION

### 2.1 Single Foam Pyramidal Absorber

The first part of this study deals with ensuring that the CFD models used are calibrated to published results. Watanabe *et al.* (2007) modeled a single pyramidal foam absorber exposed to an RF power of 399.2 (W/m<sup>2</sup>) at 6 GHz, and have further measured the temperature along the centerline of an absorber exposed to the same conditions. The computation domain used in their study (as well as the first part of this study) can be seen in Fig. 1, where a single pyramidal absorber is shown. In their study, a Finite- difference time-domain (FDTD) method along with a semi-implicit method for pressure linked equations (SIMPLE) method is used to determine the temperature distribution within a pyramidal foam absorber subjected to a 6 GHz wave. After determining this temperature distribution by solving the governing equations, a single pyramidal foam absorber is subjected to the same frequency wave with a power of approximately 400 (W/m<sup>2</sup>). The temperature is then measured along the centerline of the absorber using thermocouples.

This allows empirical results to be compared to measured results in order to validate the accuracy of the differential equations used in their empirical solution. The initial and boundary conditions for the geometry in this study are as follow: at the flow inlet  $v = 1$  (m/s) at  $x = 0$  mm,  $v = w = 0$ ,  $T = 293.15$  K. The outlet is located at  $x = 382$  mm. A constant heat flux of 400 W/m<sup>2</sup> was applied on all faces of

the pyramidal foam absorber in order to mimic the 6 GHz RF wave of Watanabe et al. (2007). It should be mentioned that COMSOL Multiphysics has the capability of coupling the RF / Electromagnetic Field Equations to the Heat Transfer / Flow Equations. During preliminary investigations into this current simulation it was decided that the large frequency of 6 GHz was not appropriate for the RF module of COMSOL, which is based on low-frequency RF theory. Hence, our simulations are standard coupled flow/energy with porous media. Consequently, the governing equations for heat and fluid flow for the porous media being solved numerically by COMSOL are as follows:

Continuity Equation:

$$\nabla \cdot \vec{V} = 0 \tag{1}$$

Assuming the air is incompressible at the flow speed considered.

Momentum Equation:

$$\rho_f \left[ \frac{1}{\varepsilon} \frac{\partial \vec{V}}{\partial t} + \frac{1}{\varepsilon} \vec{V} \cdot \frac{1}{\varepsilon} \nabla \vec{V} \right] = -\nabla p + \mu_{eff} \nabla^2 \vec{V} - \frac{\mu}{\kappa} \vec{V} - \rho C_p |\vec{V}| \vec{V} \tag{2}$$

which includes the various terms for porous flow Energy Equation:

$$(\rho C_{p,eff}) \frac{\partial T}{\partial t} = \nabla \cdot k_{eff} \nabla T + \dot{q}_{eff}'' \tag{3}$$

where  $\varepsilon$  is the volumetric porosity of the porous medium,  $\kappa$  is the porous media permeability,  $k$  is the thermal conductivity,  $\rho$  is the density,  $\mu$  is the dynamic viscosity, and the subscripts “f”, “eff” and “s” stand for fluid, effective, and solid, respectively. The effective thermal conductivity of the porous media has been investigated in previous studies Zhao (2012). In the current study, the effective thermal conductivity is found using the following correlation

$$k_{eff} = \varepsilon k_f + (1 - \varepsilon) k_s \tag{4}$$

where  $k_s$  and  $k_f$  are the thermal conductivity of the solid constituent and fluidic constituent, respectively.

For the present study, the absorber (base, pedestal, and pyramidal section) has been assumed to be composed of low density polyurethane foam, a standard industrial material used when manufacturing pyramidal foam absorbers used in anechoic chambers. The properties used in the analysis for the polyurethane foam absorber and air are listed in Table 1. The thermal conductivity of the pyramidal and pedestal part were assumed to be 0.041 (W/m-K) in agreement with the work of Watanabe et al. (2007).

The porosity, also known as the void fraction, of a porous medium is defined as the ratio of the pore volume to the total volume as shown in Eqn. (5)

$$\varepsilon = \frac{V_{pore}}{V} \tag{5}$$

**Table 1 Foam and air properties**

| Material | Property             | Value    | Units             |
|----------|----------------------|----------|-------------------|
| Foam     | Density              | 40.05    | kg/m <sup>3</sup> |
|          | Specific Heat        | 2220.0   | J/kg/K            |
|          | Thermal Conductivity | 0.041    | W/m/K             |
| Air      | Density              | 1.293    | kg/m <sup>3</sup> |
|          | Kinematic Viscosity  | 4.783E-5 | m <sup>2</sup> /s |
|          | Dynamic Viscosity    | 6.184E-5 | kg/m/s            |
|          | Thermal Conductivity | 0.0257   | W/m/K             |
|          | Specific Heat        | 1005.0   | J/kg/K            |
|          | Specific Heat Ratio  | 1.401    | -                 |

The porosity,  $\varepsilon$  can be specified when manufacturing a material, such as a pyramidal foam absorber. Similarly, permeability,  $\kappa$  is a hydraulic property of a porous media Narasimhan (2012) which measures the ease with which a fluid can move through the porous medium. This property, however, cannot be controlled as easily as porosity.

Porosity values for metal foams can be found in many papers (Bhattacharya et al. 2002; Phanikumar et al. 2002; Hsieh et al. 2004), however, to date, there has not been much work done investigating the porosity of polyurethane low density foam. The porosity values used in our current study have been taken from manufacturer reported values of pore diameter and pores per inch (PPI) for pyramidal foam absorbers used in anechoic chambers. In order to find the permeability, the Kozeny-Carman equation has been employed, which is the starting point for many permeability models (Narasimhan 2012; Xu and Yu 2008). The Kozeny-Carman equation relates the permeability to the porosity through the following equation:

$$\kappa = \frac{\varepsilon^3}{CS^2(1-\varepsilon)^2} \tag{6}$$

Where  $C$  and  $S$  are the Kozeny constant and specific surface area, respectively. The selected value of the parameter  $C$  of Eqn. (6) follows from typical values found in Burmeister (1993). Using a proposed value of  $C=5.0$  and assuming the porous media to be composed of uniform spheres of diameter  $d$  making  $S=6/d$  from Probstein (1989), Eqn. (6) becomes:

$$\kappa = \frac{d^2 \varepsilon^3}{180(1-\varepsilon)^2} \tag{7}$$

The resulting values of porosity,  $\varepsilon$  and permeability,  $\kappa$  used in this study are shown in Table 2.

## 2.2 CFD Model of 3x3 Foam Absorber Array

With our single pyramidal porous foam CFD model verified and validated to the results of Watanabe et al. (2007), a more realistic application of pyramidal foam absorbers for anechoic chambers can be investigated.

**Table 2 Porosity and permeability values**

| Quantity               | Value     | Units          |
|------------------------|-----------|----------------|
| Sphere Diameter, $d$   | 200       | microns        |
|                        | 0.00787   | in.            |
| Pores Per Inch (PPI)   | 60        | Pores/in.      |
| Porosity, $\epsilon$   | 0.472     |                |
| Permeability, $\kappa$ | 8.420E-11 | m <sup>2</sup> |

A matrix of 3x3 geometry was created with a total of nine pyramidal foam absorbers which represent a typical product sold by manufacturers. The absorbers are made of the same material as the single absorber model, as polyurethane foam is typically used in industry. The 3x3 domain can be seen in Fig. 2, where the same boundary conditions and governing equations used for the single absorber apply to the 3x3 array.

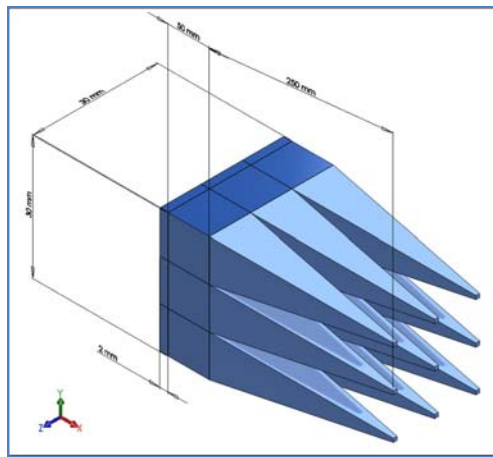


**Fig. 2. Foam absorber array.**

A parametric study was conducted on the 3x3 array geometry configuration by varying the following variables, heat flux, inlet air velocity, porosity, permeability. From this parametric study, we obtain the temperature gradient within the pyramidal foam absorber array by numerically solving the governing differential equations. This allows for an optimization study to occur, which would aid in the design of an absorber array that would meet specific criteria, without requiring the use of destructive testing.

**Table 3 Parametric study parameter values**

| Parameter              | Value(s)                                 | Units            |
|------------------------|--|------------------|
| Heat Flux, $q''$       | 400, 500, 1000, 10000, 100000            | W/m <sup>2</sup> |
| Velocity, $u$          | 1, 5, 7, 10, 100                         | m/s              |
| Porosity, $\epsilon$   | 0.472, 0.80, 0.90, 0.95                  | -                |
| Permeability, $\kappa$ | 8.4195e-11, 2.8444e-9, 1.62e-8, 7.621e-8 | m <sup>2</sup>   |

In order to confirm the results of this 3x3 model, the analytical solution proposed by Bejan (1994) for a plane wall with constant heat flux was used to validate the CFD results. The analytical solution of Bejan (1994) is being used for comparison, as there are no studies available to the authors' knowledge

to date dealing with the topic presented in this work. The analytical solution proposed by Bejan (1994) for a horizontal plane wall is given as follows:

$$Nu_x = \frac{q''x}{k(T_o(x) - T_\infty)} = 0.886Pe_x^{1/2} \quad (8)$$

In the above equation,  $q''$  is the applied heat flux,  $k$  is the thermal conductivity of the porous material (not to be mistaken as the effective thermal conductivity),  $T_o(x)$  is the wall temperature at some point,  $T_\infty$  is the temperature of the fluid-saturated porous medium, and  $Pe_x$  is the Peclet number (ratio of convection to thermal diffusivity) defined as:

$$Pe_x = \frac{U_\infty x}{\alpha} \quad (9)$$

where the thermal diffusivity is given by

$$\alpha = \frac{k_{eff}}{\rho_f C_{p,f}} \quad (10)$$

In the above equations,  $k_{eff}$  is effective thermal conductivity of the entire porous medium, whereas the density and heat capacitance are of the fluid only. Solving equation (8) for  $T_\infty$  gives us the following analytical solution:

$$T_\infty = T_o(x) - \frac{q''x}{0.866kPe_x^{1/2}} \quad (11)$$

In using Eqn. (8) to compare our CFD results of a pyramid shaped plane to that of a horizontal plane wall the author's recognize some error will be incurred. It should be mentioned here that we are using Eqn. (8) as a bounding case only, noting that to the authors' present knowledge and after conducting an exhaustive literature review, correlations for rods or cylinders for porous media heat transfer do not currently populate the database of current literature regarding this field of study.

### 3. NUMERICAL PROCEDURE

Numerical solutions to the governing partial differential equations (PDEs) shown above were found using COMSOL which employs the Galerkin Finite Element Method (FEM) to solve physical problems. Recall that the Galerkin FEM takes the weighting functions to be the same as the interpolating polynomials. This method first takes the continuous functions (differential equations) and transforms them into the weak form by multiplying the differential problem with weighting functions and then integrating by parts over the domain. Once the problem is in its weak form its residual is minimized. The resulting algebraic equations (for steady flow problems) are subsequently solved in COMSOL using the Algebraic Multigrid Method.

#### 3.1 Grid Independence Study

A grid independence study was performed on the finite element mesh. The COMSOL mesh uses tetrahedral elements with local prismatic element refinement at the wall in the region of the boundary

layers. The single absorber model was solved five different times, where all models were kept the same except for each having a different size mesh. The number of elements used to create the mesh (11,677 elements, 62,466 elements, 134,578 elements, 316,578 elements, and 375,024 elements) was varied for each of the five models in order to determine the most efficient mesh size (in terms of computation time vs. change in resulting temperatures). As seen in tableTable 4, a mesh size of 316,578 elements was chosen as ideal as any greater number of elements used did not produce a significant change of resulting temperatures.

**Table 4 Grid independent study**

| Number of Elements | Maximum Model Temperature [K] | Percent Change |
|--------------------|-------------------------------|----------------|
| 11,677             | 321.8                         | -              |
| 62,466             | 339.1                         | 5.4%           |
| 134,578            | 344.0                         | 1.4%           |
| 316,578            | 345.2                         | 0.3%           |
| 375,024            | 345.7                         | 0.1%           |

### 3.2 CFD Model Verification and Validation

The single pyramidal absorber CFD model used in this study has been calibrated to the results of Watanabe et al. (2007) for high power injection in a foam absorber. The pyramidal absorber is composed of a base, a pedestal, and a pyramidal section, where the high power electromagnetic wave was approximated within COMSOL v4.3a using a constant heat flux, 400 (W/m<sup>2</sup>), on the faces of the absorber. Further, in order to realize the cooling strategy proposed, ambient air was blown parallel along the length of the absorber, beginning from the base, to help aid in the removal of heat generated by the heat flux.

As shown in Fig. 3. the results of the current study were found to be in qualitative and quantitative agreement (within ±18% of the calculated results) with the calculated results presented by Watanabe et al. (2007). In Fig. 3 the calculated results of Watanabe et al. (2007) versus the current CFD results are shown for a single foam absorber which is positioned at the center of the y-z plane of the array. In addition to numerical predictions, Watanabe et al. (2007) also provide measured values for the temperature distribution along the centerline of the pyramidal foam absorber. The values have been averaged from the work of Watanabe et al. (2007) and compared to the results of this study.

Fig. 4 shows the measured results of Watanabe et al. (2007) versus the current CFD results for a single foam absorber which is positioned at the center of the y-z of the array. From Fig. 4, the present study CFD results are found to in agreement with the measured data of Watanabe et al. (2007), and are within 14% of the measured values for all data points.

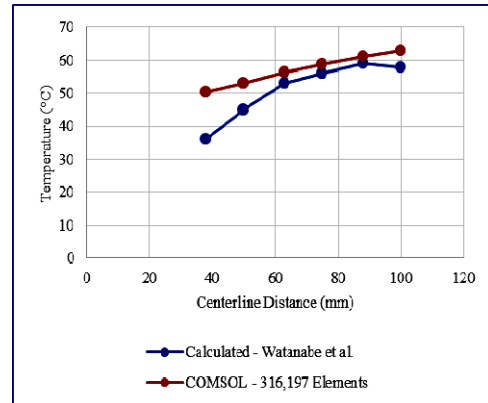


**Fig. 3. Temperature distribution numerical data of Watanabe et al. (2007) versus current CFD along the centerline of the pyramidal foam absorber.**

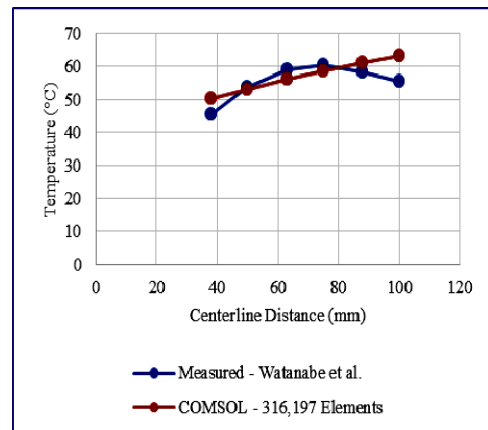


**Fig. 4. Temperature distribution measured data of Watanabe et al. (2007) versus current CFD along the centerline of the pyramidal foam absorber.**

## 4. RESULTS AND DISCUSSION

### 4.1 Single Foam Absorber Study

The surface temperature profile for the single absorber and distribution is shown in Fig. 5 and Fig. 6, respectively, while the velocity profile along the centerline of the pyramidal foam absorber is shown in Fig. 7. In Fig. 6 the plotted results are shown for a single foam absorber which is positioned at the center of the y-z plane of the array. As can be seen in Fig. 5, the maximum temperature reached is 73°C, which is well under the recommended operating temperature of 200°C for commercial, low-density polyurethane foam. This simulation shows that the single pyramidal absorber will be able to withstand the operating temperatures seen throughout its life if kept within the specified operating characteristics. The entry length region results of Fig. 6 are seen to be in qualitative agreement with the study performed by Sozen and Kuzay (1996).



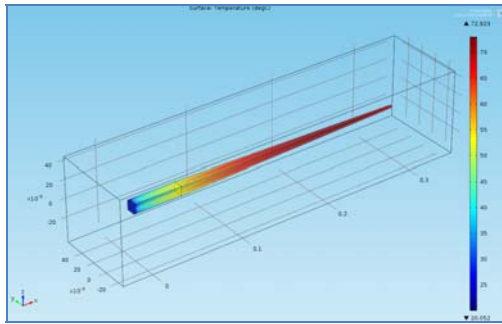


**Fig. 5. Surface temperature of single pyramidal foam absorber.**

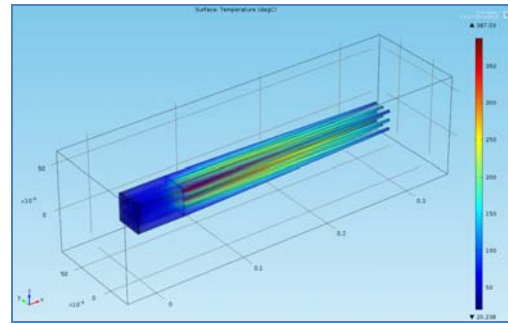


**Fig. 8. Surface temperature of 3x3 pyramidal foam absorber array.**

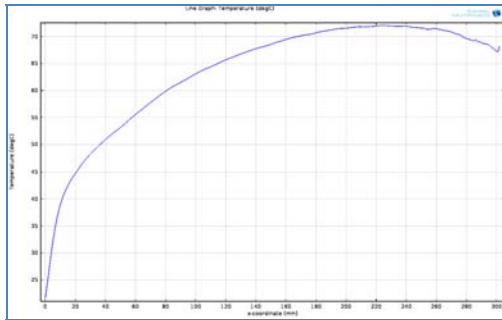


**Fig. 6. Centerline temperature distribution of single pyramidal foam absorber.**

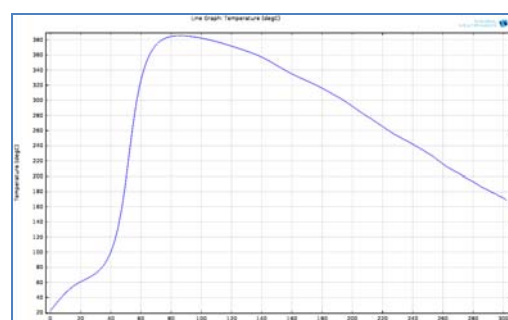


**Fig. 9. Centerline temperature distribution of 3x3 pyramidal foam absorber array.**

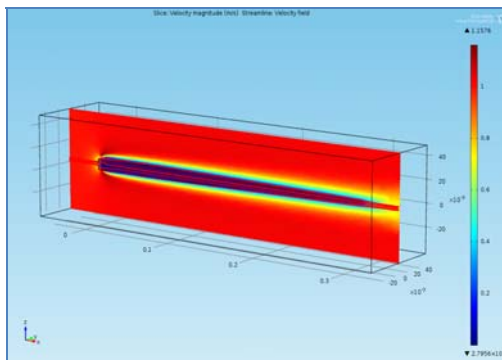


**Fig. 7. Velocity profile with streamlines (in red).**

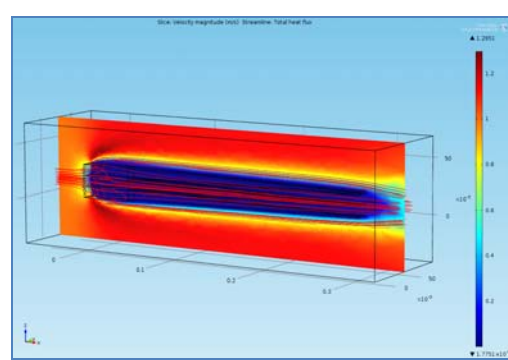


**Fig. 10. Velocity profile with streamlines (in red).**

#### 4.2 Pyramid Array Study

The second part of this study looked into simulating a real world application using a 3x3 array of pyramidal foam absorbers for anechoic chambers. A 3x3 array was built using the same model as in the first part of this study. The surface temperature profile and distribution is shown in Fig. 8 and Fig. 9, respectively, while the velocity profile along the centerline of the pyramidal foam absorber is given in Fig. 10. The simulations for the 3x3 absorber array, modeled exactly as the single absorber simulations, show that the max temperature reached would be 387°C, resulting in the failure of the absorber array. The temperature on the outside of the array is 150°C is within the maximum allowable temperature for the foam, however, the center of the array reaches 387°C as shown in Fig. 8. As the ambient air is blown around the array, only the surface is allowed to dissipate heat, while the center does not have enough air flow to remove the generated heat.

A Parametric study with the controlling parameters of heat flux ( $W/m^2$ ), fluid velocity (m/s), porosity (-), and permeability ( $m^2$ ) was conducted in order to determine what conditions were necessary to keep the absorber array within the maximum allowable operating conditions. The parametric study also shed some light on the relationship between porosity and temperature distribution. Figure 11 shows temperature along the x-axis for a permeability of  $\kappa=8.4195 \times 10^{-11}$  held constant as the porosity varies from  $\epsilon=0.42, 0.80, 0.90, 0.95$ . As seen in Fig. 11, at a fixed x-location the higher porosity values result in higher temperatures. This trend can be explained by looking at Eqn. (4) for the effective thermal conductivity, where the total effective thermal conductivity is found from the arithmetic mean of both the solid and fluid constituent using the volume fraction (porosity) as the weighting factor. Given that in this study, the fluid is taken to be air which has a thermal conductivity almost 63% less than that of the solid media (polyurethane), the higher the porosity of the

media would equate to a smaller overall effective thermal conductivity for the porous media. This lower thermal conductivity would mean that less heat can be removed from the media, and would equate to greater temperature distribution.

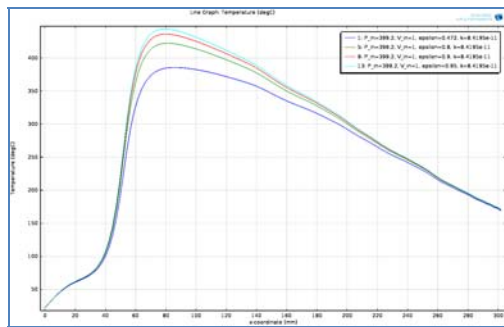


**Fig. 11. Temperature distribution along centerline for varying porosities.**

Based on the parametric study performed, the best case operating conditions which may allow the pyramidal foam absorber to stay within the max allowable temperature are as follows: porosity,  $\epsilon = 0.472$ ; permeability,  $\kappa = 8.4195 \times 10^{-11} \text{ m}^2$ ; inlet air cooling velocity = 50 m/s. Fig. 12 shows the temperature profile within the pyramidal foam absorber array when using these parameters.

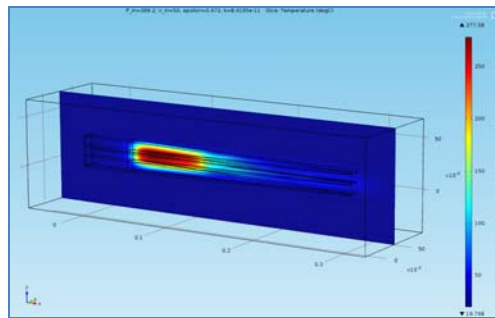


**Fig. 12. Surface temperature of 3x3 pyramidal foam absorber array using best case parameters.**

Next, the analytical solution proposed by Bejan (1994) (herein included as Eqn. (11)) was used to compare the results obtained from the present CFD simulations and the heat transfer theory. In order to evaluate Eqn. (11),  $T_o(x)$  was obtained from COMSOL and used in Eqn. (8) to obtain the centerline temperature of the pyramidal foam absorber. The correlated centerline temperature was then compared to the actual centerline temperature as taken from the CFD simulations and found to be on average within 11% of the analytical solution proposed by Bejan (1994). Fig. 13 shows the comparison of the two centerline temperatures. Once again, it should be mentioned that the use of Eqn. (11) of Bejan (1994) is taken as a bounding case only in the absence of no rod or cylindrical geometry correlation available in the present literature. In addition, as mentioned earlier in this manuscript our verification and validation using the data of Watanabe et al. (2007) shows that the current CFD model created is within 20% of the measured results.

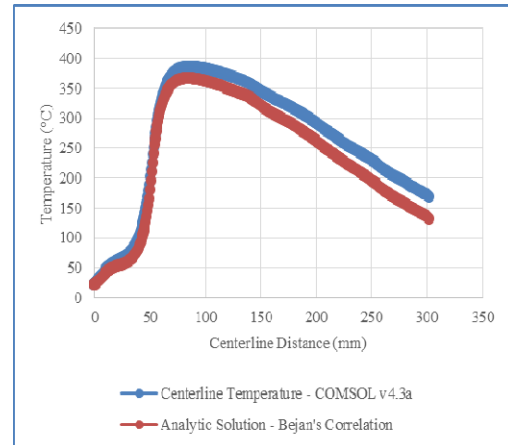


**Fig. 13. Centerline temperature distribution comparison between CFD and theory.**

As is evident in Fig. 13, the results of our CFD simulations are in close agreement with those predicted by theory. Furthermore, the results of Fig. 13 are found to be in qualitative agreement with the study of Tada and Ichimiya (2007) for heat transfer in a saturated circular tube with constant heat flux. Comparing our maximum temperature of Fig. 13 to the correlation of Tada and Ichimiya (2007) for the wall temperature defined in Tada and Ichimiya (2007) as follows:

$$T = T_o + \frac{\theta q_w R}{k_{eff}} \quad (12)$$

where, as detailed in Tada and Ichimiya (2007),  $\theta$  denotes the non-dimensional wall temperature,  $q_w$  denotes the wall heat flux,  $R$  is the radius of the tube, and  $k_{eff}$  is the effective thermal conductivity of the tube. We find that our maximum temperature in Fig. 13 corresponds to the case of Tada and Ichimiya (2007) for the limit of a solid pipe

### 3. CONCLUSION

In this study, heat transfer and fluid flow within a pyramid array porous media domain were modeled with CFD software and the results compared to previous works. The CFD software uses the Brinkman-Darcy model with an effective thermal conductivity to account for the porous nature of the medium. The first part of this study focused on calibrating and validating the simulation model to the work of Watanabe et al. (2007). Our verification and validation using the data of Watanabe et al. (2007) shows that the current CFD model created is within 20% of the measured results of Watanabe et al. (2007). Once our CFD model of a single porous foam pyramidal absorber model was validated, a real world application for pyramidal foam absorbers was modeled, whereby a 3x3 array of pyramidal absorbers was simulated. The results of this second part of this current study were compared to the work of Bejan (1994), where the results were found to be within 11% of the theoretical correlation for the Nusselt number along the centerline of the 3x3 array. The results of a comprehensive parametric study involving the heat flux, fluid velocity, media porosity, and permeability showed that there is a

fundamental underlying relationship between porosity and the temperature distribution within the porous media. That being, the more porous a media is, the more dependent the effective thermal conductivity would be on the thermal conductivity of the fluid. If the fluid is air, which has a very low thermal conductivity, the effective thermal conductivity is decreased as the porosity increases, thus tending to stifle the overall heat transfer. Further investigation in this topic could expand on this work by exploring different cooling methods for removing the heat generated within the pyramidal foam absorber. Another topic of interest would be examining the relationship between porosity and temperature distribution within the porous medium. If this property could be controlled through greater precision in manufacturing processes, a very efficient porous medium could be created which would find application in foam based pyramid absorber systems currently limited by high temperatures.

#### ACKNOWLEDGEMENTS

The authors of this paper would like to thank Dr. Angela Shih, Chair of Mechanical Engineering at Cal Poly Pomona for continued support.

#### REFERENCES

- Bejan, A. (1994). *Convection heat transfer*. New York, NY: Wiley-Interscience.
- Bhattacharya, A., V. V. Calmidi and R. L. Mahajan, (2002). Thermophysical properties of high porosity metal foams. *International Journal of Heat and Mass Transfer* 45 (5), 1017-1031.
- Boomsma, K. and D. Poulikakos (2000). On the effective thermal conductivity of a three-dimensionally structured fluid-saturated metal foam. *International Journal of Heat and Mass Transfer* 44(4), 827-836.
- Burmeister, L. C. (1993). *Convection heat transfer*. New York, NY: Wiley-Interscience.
- Cekmer, O., M. Mobedi, B. Ozerdem and I. Pop, (2012). Fully developed forced convection in a parallel plate channel with a centered porous layer. *Transport in Porous Media* 93 (1), 179-201.
- Dukhan, N. and K. Chen (2007). Heat transfer measurements in metal foam subjected to constant heat flux. *Experimental Thermal and Fluid Science* 32(2), 624-631.
- Ghosh, I. (2009). Heat transfer correlation for high-porosity open-cell foam. *International Journal of Heat and Mass Transfer* 52(5-6), 1488-1494.
- Hsieh, W. H., J. Y. Wu, W. H. Shih and W. C. Chiu (2004). Experimental investigation of heat-transfer characteristics of aluminum-foam heat sinks. *International Journal of Heat and Mass Transfer* 47(23), 5149-5157.
- Kopanidis, A., A. Theodorakakos, E. Gavaises and D. Bouris (2010). 3d numerical simulation of flow and conjugate heat transfer through a pore scale model of high porosity open cell metal foam. *International Journal of Heat and Mass Transfer* 53(11-12), 2539-2550.
- Narasimhan, A. (2012). *Essentials of Heat and Fluid Flow in Porous Media*. Boca Raton, FL: CRC Press.
- Phanikumar, M. S. and R. L. Mahajan (2002). Non-Darcy natural convection in high porosity metal foams. *International Journal of Heat and Mass Transfer* 45(18), 3781-3793.
- Probstein, R. F. (1989). *Physicochemical hydrodynamics: An introduction*. New Jersey: John Wiley & Sons.
- Sozen, M. and T. M. Kuzay (1996). Enhanced heat transfer in round tubes with porous inserts. *International Journal of Heat and Fluid Flow* 17, 124-129.
- Tada, S. and K. Ichimiya (2007). Analysis of laminar dissipative flow and heat transfer in a porous saturated circular tube with constant wall heat flux. *International Journal of Heat and Mass Transfer* 50, 2406-2413.
- Watanabe, S., T. Sasagawa, O. Hashimoto and T. Saito (2007). Study of temperature distribution of a pyramidal EM-wave absorber under high power injection. *Proceedings from the 37th European Microwave Conference*, Munich, Germany.
- Xu, P. and C. Yu (2008). Developing a new form of permeability and Kozeny-Carman constant for homogeneous porous media by means of fractal geometry. *Advances in Water Resources* 31(1), 74-81.
- Zhao, C. Y. (2012). Review on thermal transport in high porosity cellular metal foams with open cells. *International Journal of Heat and Mass Transfer* 55(13-14)
- Zhao, C. Y., T. J. Lu and H. P. Hodson (2005). Natural convection in metal foams with open cells. *International Journal of Heat and Mass Transfer* 48(12), 2452-2463.